

Template-Directed Syntheses, Spectroscopic Properties, and Electrochemical Behavior of $[n]$ Catenanes

Peter R. Ashton,^[a] Virna Baldoni,^[b] Vincenzo Balzani,^{*,[b]} Christian G. Claessens,^[a] Alberto Credi,^[b] H. D. Andreas Hoffmann,^[a] Francisco M. Raymo,^[c] J. Fraser Stoddart,^{*,[c]} Margherita Venturi,^{*,[b]} Andrew J. P. White,^[d] and David J. Williams^{*,[d]}

Keywords: Catenanes / Cyclophanes / Electrochemistry / Electronic spectroscopy / Template-directed synthesis

Catenanes composed of two, three, five, or seven interlocked macrocycles have been synthesized in yields ranging from 1 to 30%. Their template-directed syntheses rely on a series of cooperative noncovalent bonding interactions between π -electron rich 1,5-dioxynaphthalene ring systems and π -electron deficient bipyridinium units which are incorporated within the macrocyclic components. The interlocked structure associated with one of the [3]catenanes was demonstrated unequivocally by single crystal X-ray analysis which also revealed the formation of polar stacks stabilized by intermolecular $[\pi \cdots \pi]$ interactions. The number of interlocked components of each catenane was determined by liquid secondary ion, matrix-assisted laser desorption ionization/time-

of-flight, and/or electrospray mass spectrometries. The absorption spectra, emission spectra, and electrochemical properties of the macrocyclic components and of the catenanes have been investigated. Two kinds of charge-transfer absorption bands (intramolecular in the cyclophanes containing electron-donor and electron-acceptor units, intercomponent in the catenanes) have been found. Such charge-transfer excited states are responsible for the quenching of the potentially fluorescence units of the cyclophanes, and of the crown ethers in the catenanes. Charge-transfer electronic interactions are also evidenced by the electrochemical behavior. Correlations among the redox potentials of the various compounds are reported and discussed.

Introduction

The tetracationic cyclophanes 1^{4+} – 3^{4+} incorporate^[1] (Figure 1) complementary π -electron deficient and π -electron rich recognition sites. As a result of $[\pi \cdots \pi]$ stacking interactions,^[2] these self-complementary^[3] molecules can recognize one or more identical copies of themselves to self-assemble into well-defined supramolecular arrays in the solid state^[1] and on solid surfaces.^[4] In addition, they can bind^[1,5] π -electron rich guests inside their cavities, once again, as a result of $[\pi \cdots \pi]$ stacking interactions which can be supplemented by $[C-H \cdots O]$ and $[C-H \cdots \pi]$ interactions.^[6,7] This recognition motif has been employed to synthesize^[5,8] three [3]catenanes^[9] each incorporating the tetra-

cationic cyclophane 2^{4+} and two identical dioxyarene-based macrocyclic polyethers. In order to explore further the ability of these self-complementary cyclophanes to form $[n]$ catenanes, we have envisaged the possibility of interlocking the tetracationic cyclophanes 1^{4+} – 3^{4+} with the macrocyclic polyethers **4**, **5**, and **6** incorporating^[10] (Figure 1) two, three, and four 1,5-dioxynaphthalene recognition sites.^[11] Here, we report (i) the template-directed syntheses of three [2]catenanes, five [3]catenanes, one [5]catenane, and one [7]catenane incorporating the macrocyclic components illustrated in Figure 1, (ii) the X-ray crystal structure of a [3]catenane incorporating the tetracationic cyclophane 3^{4+} and two macrocyclic polyethers **4**, (iii) the liquid secondary ion, the matrix-assisted laser desorption ionization/time-of-flight, and the electrospray mass spectrometric investigations of all ten catenanes, (iv) the absorption spectra of the cyclophanes 2^{4+} and 3^{4+} , the macrocyclic polyethers **5** and **6**, and four of the [3]catenanes, (v) the fluorescence spectra of the macrocyclic polyethers **5** and **6**, and (vi) the electrochemical properties of the cyclophanes 2^{4+} and 3^{4+} , the macrocyclic polyether **6**, and four of the [3]catenanes.

Results and Discussion

Synthesis

Reaction of the dibromides **7**, **8**, and **9** with the corresponding bis(hexafluorophosphate) salts **10** · 2 PF₆,

[‡] Part 56: R. Ballardini, V. Balzani, W. Dehaen, A. E. Dell'Erba, F. M. Raymo, J. F. Stoddart, M. Venturi, *Eur. J. Org. Chem.* **2000**, 591–602.

[a] School of Chemistry, University of Birmingham, Edgbaston, Birmingham, B15 2TT (UK)

[b] Dipartimento di Chimica "G. Ciamician", Università di Bologna, via Selmi 2, 40126 Bologna (Italy)
Fax: (internat.) +39-051/209-9456
E-mail: vbalzani@ciam.unibo.it

[c] Department of Chemistry and Biochemistry, University of California, Los Angeles, 405 Hilgard Avenue, Los Angeles, CA 90095-1569 (USA)
Fax: (internat.) +1-310/206-1843
E-mail: stoddart@chem.ucla.edu

[d] Department of Chemistry, Imperial College, South Kensington, London, SW7 2AY (UK)
Fax: (internat.) +44-171/594-5835

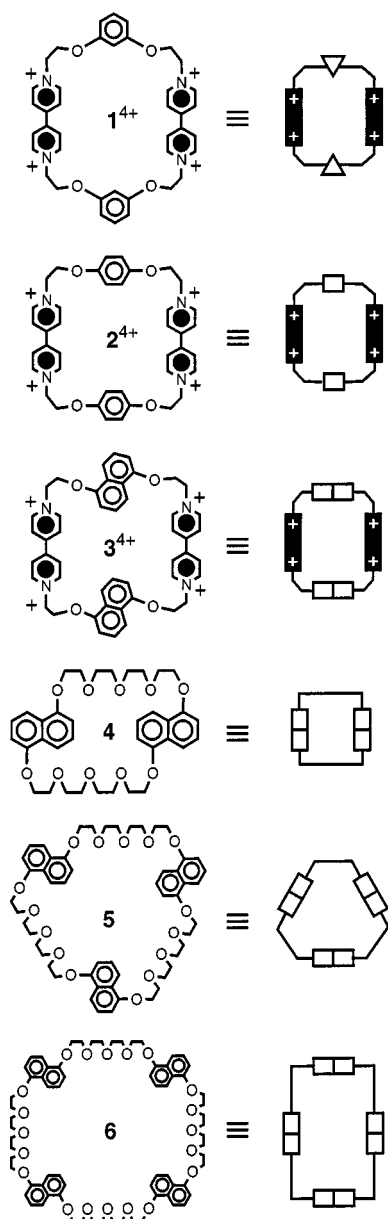
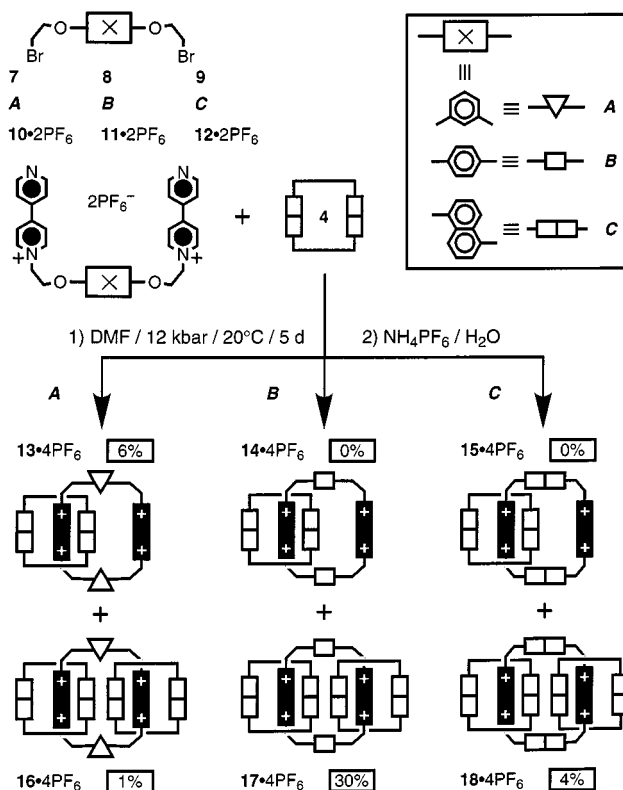
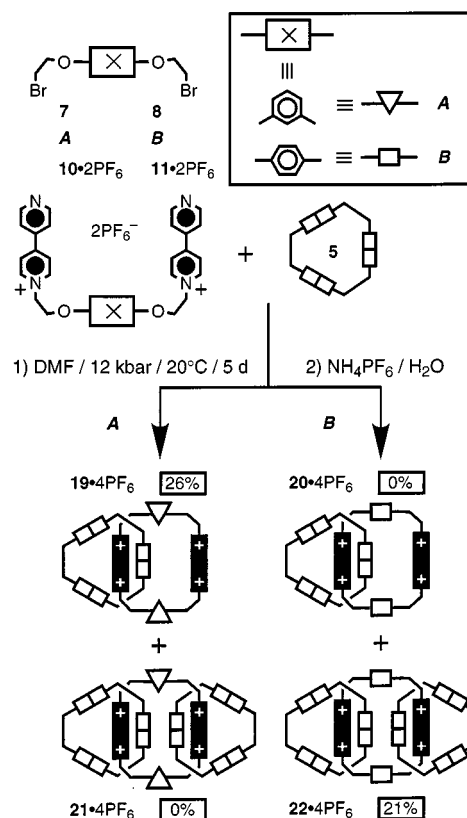


Figure 1. The bipyridinium-based tetracationic cyclophanes $1 \cdot 4 \text{ PF}_6$, $2 \cdot 4 \text{ PF}_6$, and $3 \cdot 4 \text{ PF}_6$, and the 1,5-dioxynaphthalene-based macrocyclic polyethers **4–6**

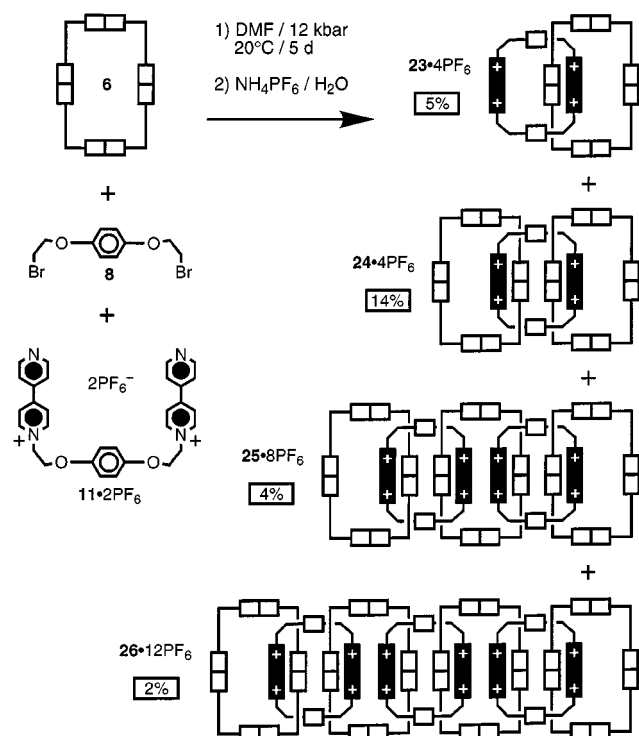
$11 \cdot 2 \text{ PF}_6$, and $12 \cdot 2 \text{ PF}_6$, respectively, in the presence of the macrocyclic polyether **4** afforded^[12] (Scheme 1) the [3]catenanes $16 \cdot 4 \text{ PF}_6$ (1%), $17 \cdot 4 \text{ PF}_6$ (30%), and $18 \cdot 4 \text{ PF}_6$ (4%), respectively, after precipitation with an excess of NH_4PF_6 . In the case of the *m*-phenylene-containing compounds **7** and $10 \cdot 2 \text{ PF}_6$, the [2]catenane $13 \cdot 4 \text{ PF}_6$ was also isolated in a yield of 6%. Reaction of the dibromides **7** and **8** with the corresponding bis(hexafluorophosphate) salts $10 \cdot 2 \text{ PF}_6$ and $11 \cdot 2 \text{ PF}_6$, respectively, in the presence of the larger macrocyclic polyether **5** afforded (Scheme 2) the [2]catenane $19 \cdot 4 \text{ PF}_6$ (26%) and the [3]catenane $22 \cdot 4 \text{ PF}_6$ (21%), respectively. Reaction of the dibromide **8** with $11 \cdot 2 \text{ PF}_6$ in the presence of the even larger macrocyclic polyether **6** afforded (Scheme 3) the [2]catenane $23 \cdot 4 \text{ PF}_6$, the [3]catenane $24 \cdot 4 \text{ PF}_6$, the [5]catenane



Scheme 1. The template-directed syntheses of the [2]catenane $13 \cdot 4 \text{ PF}_6$ and of the [3]catenanes $16 \cdot 4 \text{ PF}_6$, $17 \cdot 4 \text{ PF}_6$, and $18 \cdot 4 \text{ PF}_6$



Scheme 2. The template-directed syntheses of the [2]catenane $19 \cdot 4 \text{ PF}_6$ and of the [3]catenane $22 \cdot 4 \text{ PF}_6$



Scheme 3. The template-directed syntheses of the [2]catenane **23** • 4 PF_6 , the [3]catenanes **24** • 4 PF_6 , the [5]catenane **25** • 8 PF_6 , and the [7]catenane **26** • 2 PF_6

25 • 8 PF_6 , and the [7]catenane^[13] **26** • 12 PF_6 in yields of 5, 14, 4, and 2%, respectively.

X-Ray Crystallography

The X-ray analysis of the [3]catenane **18** • 4 PF_6 confirms (Figure 2) the interlocked structure of this molecule. The overall molecular symmetry approximates to C_2 , with the two-fold axis passing through the center of the tetracationic cyclophane and normal to its mean plane. However, this axis is not coincident with the crystallographic b axis. The

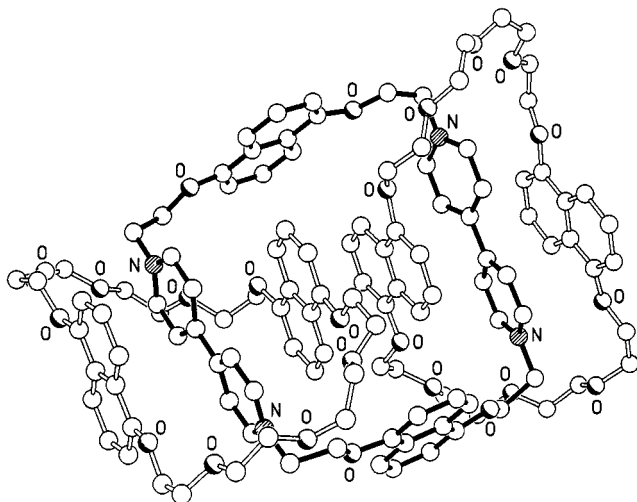


Figure 2. Ball-and-stick representation of the geometry adopted by the [3]catenane **18**⁴⁺ in the solid state

structure is stabilized by $[\pi \cdots \pi]$ stacking between the bipyridinium units and the sandwiching 1,5-dioxynaphthalene ring systems and between the pair of “inside” 1,5-dioxynaphthalene ring systems. The interplanar separations range between 3.30 and 3.52 Å, the largest separation being between the pair of “inside” 1,5-dioxynaphthalene ring systems. The tetracationic cyclophane has a twisted conformation with the $[\text{N} \cdots \text{N}]$ axes of the two bipyridinium units inclined by 32°. The principal orientations of the 1,5-dioxynaphthalene ring systems in each macrocyclic polyether are not superimposable, as is also the case for the pair of “inside” 1,5-dioxynaphthalene ring systems. There is evidence for “pedaling” of one of the “alongside” 1,5-dioxynaphthalene ring systems. The ratio between the occupancies of the two orientations is ca. 60:40 and the major occupancy is the one illustrated in Figure 2. Although there is evidence for intracatenane $[\text{C}-\text{H} \cdots \text{O}]$ hydrogen bonds, we have not analyzed them in detail as a result of the limited accuracy of the structure. On the other hand, $[\text{C}-\text{H} \cdots \pi]$ interactions between the “inside” 1,5-dioxynaphthalene ring systems and their counterparts in the tetracationic cyclophane appear to be absent. Glide-related molecules form polar [ABAB] stacks (Figure 3) with a mean interplanar separation between adjacent “alongside” 1,5-dioxynaphthalene ring systems of ca. 3.76 Å. There are no stacking interactions involving the 1,5-dioxynaphthalene ring systems of the tetracationic cyclophane.

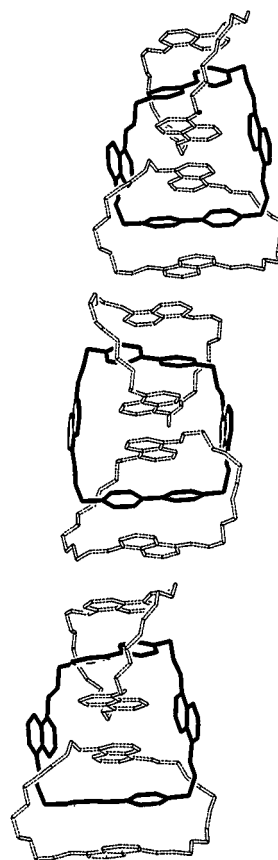


Figure 3. One of the polar stacks formed by the [3]catenane **18**⁴⁺ in the solid state

Mass Spectrometry

The [2]catenanes and the [3]catenanes were characterized (Table 1) by liquid secondary ion mass spectrometry (LSIMS). In all instances, the spectra revealed peaks at m/z values for $[M - \text{PF}_6]^+$, $[M - 2 \text{PF}_6]^+$, and $[M - 3 \text{PF}_6]^+$, corresponding to the losses of one, two, and three hexafluorophosphate counterions, respectively. For the [3]catenanes **16** · 4 PF_6 and **24** · 4 PF_6 , peaks at m/z values for $[M - 4 \text{PF}_6]^+$, corresponding to the loss of four hexafluorophosphate counterions were also observed. The spectra of the [3]catenane **18** · 4 PF_6 and of the [2]catenane **19** · 4 PF_6 revealed additionally peaks at m/z values for $[M]^+$ corresponding to the molecular ions.

The [2]catenane **23** · 4 PF_6 and the [3]catenane **24** · 4 PF_6 were also analyzed by matrix-assisted laser desorption ionization/time-of-flight mass spectrometry (MALDI-TOFMS). For the [2]catenane **23** · 4 PF_6 , peaks at m/z values of 2201, 2057, and 1913 for $[M - 2 \text{PF}_6]^+$, $[M - 3 \text{PF}_6]^+$, and $[M - 4 \text{PF}_6]^+$, corresponding to the losses of two, three, and four hexafluorophosphate counterions, respectively, were observed. The spectrum of the [3]catenane **24** · 4 PF_6 revealed peaks at m/z values of 3335 and 3191 for $[M - 3 \text{PF}_6]^+$ and $[M - 4 \text{PF}_6]^+$, corresponding to the losses of three and four hexafluorophosphate counterions, respectively.

The [5]catenane **25** · 8 PF_6 and the [7]catenane **26** · 12 PF_6 were characterized by electrospray mass spectrometry (ESMS). For comparison, the [2]catenane **23** · 4 PF_6 and the [3]catenane **24** · 4 PF_6 , which incorporated the same macrocyclic components of **25** · 8 PF_6 and **26** · 12 PF_6 , were also investigated by ESMS. The spectra revealed peaks at m/z values corresponding to singly and multiply charged ions derived from the consecutive losses of one to three hexafluorophosphate counterions for **23** · 4 PF_6 , two to four hexafluorophosphate counterions for **24** · 4 PF_6 , three to eight hexafluorophosphate counterions for **25** · 8 PF_6 , and four to ten hexafluorophosphate counterions for **26** · 12 PF_6 . For the [3]catenane **24** · 4 PF_6 , peaks at m/z values of 2868, 2680, and 2367 for $[4 M - 5 \text{PF}_6]^{5+}$, $[3 M - 4 \text{PF}_6]^{4+}$, and $[2 M - 3 \text{PF}_6]^{3+}$ corresponding to tetrameric, trimeric, and dimeric species, respectively, were also observed.

Absorption and Emission Properties

Figure 4 shows the compounds whose absorption and emission spectra have been examined. In addition to new compounds, for comparison purposes, we have also taken into consideration results on the previously reported^[14] macrocyclic polyether **4**, as well as examined the previously described^[15,16] macrocyclic polyether **5**, cyclophane **27**⁴⁺, [3]catenane **29**⁴⁺, and [3]catenane **28**⁴⁺. The absorption and emission properties of all the compounds investigated are summarized in Table 2.

Macrocyclic Polyethers: The absorption and fluorescence spectra of the macrocyclic polyethers **4**, **5**, and **6** (see, e.g., Figure 5) show the well-known bands for their 1,5-dioxynaphthalene chromophoric units.^[14a] In all cases, the absorption maximum, emission maximum, fluorescence quantum yield, and excited state lifetime are practically the same as in 1,5-dimethoxynaphthalene (Table 2).

Cyclophanes: Cyclophanes **2**⁴⁺ and **3**⁴⁺ are interesting species since they contain both electron-donor and electron-acceptor units. Besides the bands related to the separated chromophoric units, their absorption spectra (Figure 6) show low-intensity, broad bands in the 350–450 nm region that can be assigned to charge-transfer (CT) transitions from the electron-rich dioxybenzene or dioxynaphthalene units to the electron-deficient bipyridinium units. This band is also present in cyclophane **27**⁴⁺. The maximum of the CT band moves to higher energies along the series **3**⁴⁺, **2**⁴⁺, **27**⁴⁺ (Table 2; Figure 6, inset), in agreement with the decreasing electron donor power, as measured by the oxidation potentials of 1,5-dimethoxynaphthalene, 1,4-dimethoxybenzene, and biphenyl.^[17] A more elaborated discussion is not possible because of the different flexibility of the three cyclophanes. The fluorescence of the dioxynaphthalene, dioxybenzene, and biphenylene units cannot be observed because of the presence of the low energy CT levels.

[3]Catenanes: The absorption spectra of the [3]catenanes are characterized by the presence of a moderately intense, broad band in the 500–600 nm region (Table 2; Figure 6, inset) which can be attributed to the intercomponent CT transitions between the electron-rich units of the two macrocyclic polyethers and the electron-deficient bipyridinium units of the cyclophane. The intramolecular CT bands of

Table 1. Liquid secondary ion mass spectrometric (LSIMS) data for the [2]catenanes **13** · 4 PF_6 , **19** · 4 PF_6 , and **23** · 4 PF_6 and for the [3]catenanes **16** · 4 PF_6 , **17** · 4 PF_6 , **18** · 4 PF_6 , **22** · 4 PF_6 , and **24** · 4 PF_6 . The spectra were recorded on a VG ZabSpec mass spectrometer using 3-nitrobenzyl alcohol as matrix. The measured masses correspond to the centroids of unresolved isotopic distributions.

Catenane	$[M]^+$	$[M - \text{PF}_6]^+$	$[M - 2 \text{PF}_6]^+$	$[M - 3 \text{PF}_6]^+$	$[M - 4 \text{PF}_6]^+$
13 · 4 PF_6	[a]	1711	1566	1421	[a]
16 · 4 PF_6	[a]	2349	2204	2059	1913
17 · 4 PF_6	[a]	2347	2202	2057	[a]
18 · 4 PF_6	2594	2449	2304	2159	[a]
19 · 4 PF_6	2175	2030	1885	1739	[a]
22 · 4 PF_6	[a]	2983	2838	2693	[a]
23 · 4 PF_6	[a]	2349	2204	2059	[a]
24 · 4 PF_6	[a]	3621	3477	3332	3186

[a] Not observed.

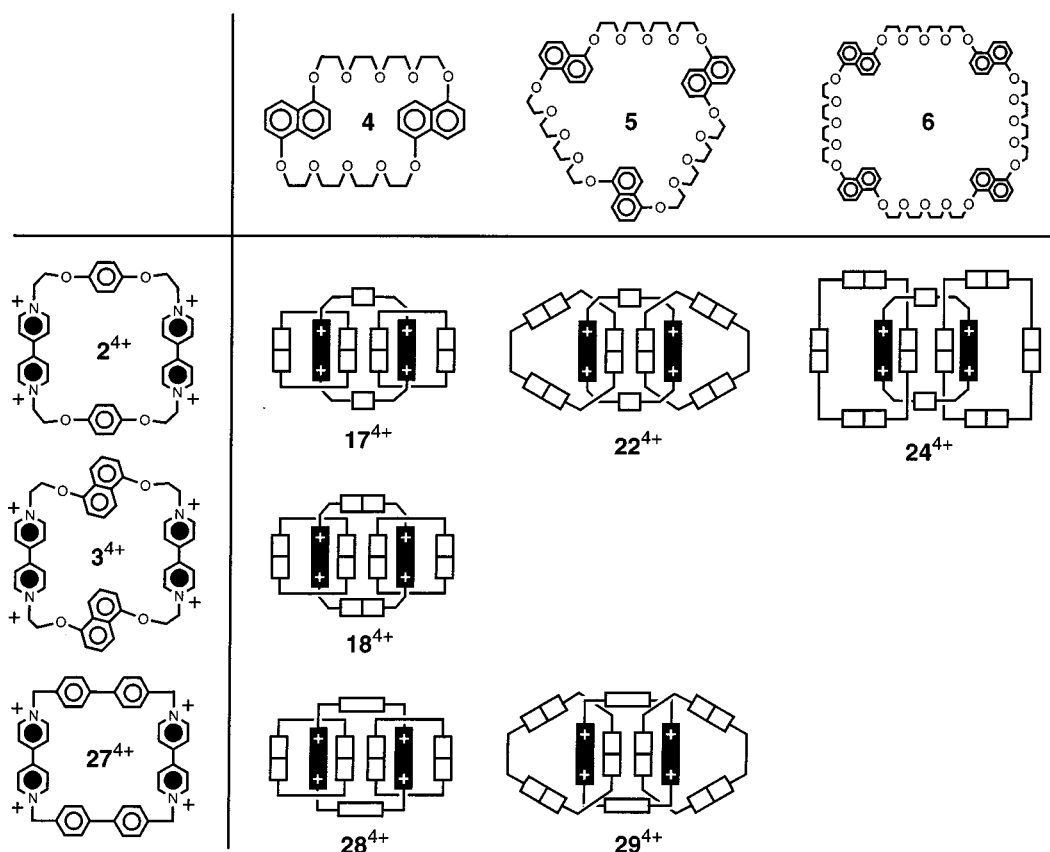


Figure 4. Representation of the macrocyclic polyether, cyclophanes, and catenanes whose absorption spectra, luminescence properties, and electrochemical behavior have been discussed

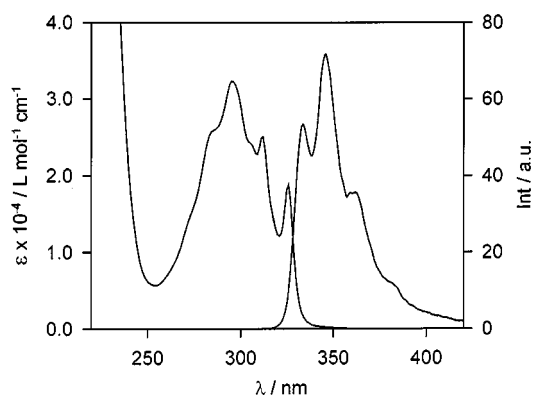


Figure 5. Absorption (left) and fluorescence (right) spectra of macrocyclic polyether **6** in MeCN at 298 K. The fluorescence spectrum was obtained with 295 nm excitation

the cyclophanes cannot be seen, presumably because they are hidden by the tail of the perturbed macrocyclic polyether bands. It should be noted that the maximum of the intercomponent CT band lies at shorter wavelength in the case of the catenanes involving macrocyclic polyethers **5**, suggesting that the donor-acceptor interaction is disfavored by the geometry of this polyether.

Electrochemistry

The electrochemical data obtained for the compounds investigated are summarized in Table 2. The reference elec-

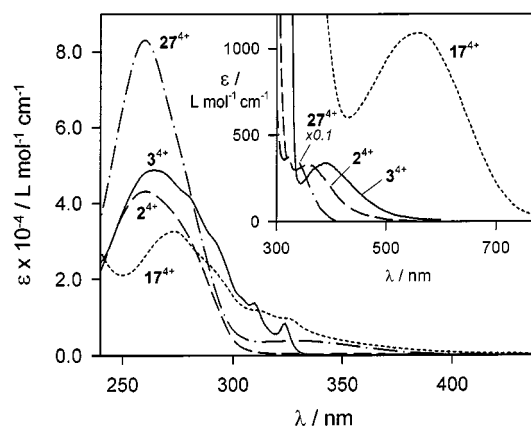
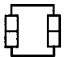

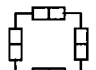







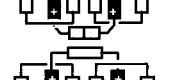



Figure 6. Absorption spectra (MeCN, 298 K) of cyclophanes **2**⁴⁺, **3**⁴⁺, and **27**⁴⁺, and of [3]catenane **17**⁴⁺. The inset shows a magnification of the charge-transfer bands

troactive groups are the electron-deficient 1,1'-dimethyl-4,4'-bipyridinium dication which undergoes^[18] two, fully reversible one electron-reduction processes at -0.43 and -0.84 V, and the electron-rich 1,5-dimethoxynaphthalene and 1,4-dimethoxybenzene compounds which undergo^[18] a poorly reversible one-electron oxidation at $+1.11$ and $+1.31$ V, respectively. Such processes are also found in the derivatives of these parent compounds, but at potential values that depend on the nature of the substituents and on structural factors. For example, cyclobis(paraquat-*p*-phenylene) un-

Table 2. Absorption, fluorescence, and electrochemical data (MeCN, 298 K)

Compound	Absorption		Fluorescence			Electrochemistry ^[a]	
	λ_{\max} (nm)	ϵ (M ⁻¹ cm ⁻¹)	$\lambda_{\max}^{[b]}$ (nm)	$\Phi^{[c]}$	τ (ns)	Reduction	Oxidation
1,5-dimethoxynaphthalene ^[d]	295	8500	328	0.38	7.5	—	+1.11 ^[e]
4 ^[f] 	295	17600	346	0.26	7.2	—	+1.05 ^[e] ; +1.15 ^[e]
5 	295	26700	346	0.34	6.8	—	+0.98 ^[e,g] ; +1.15 ^[e,g] ; +1.25 ^[e,g]
6 	295	33200	346	0.30	7.1	—	+0.98 ^[e] ; +1.10 ^[e,h]
24 ⁺ 	259 337	43200 360	—	—	—	−0.35 (2); −0.80 (2)	+1.51 (2)
34 ⁺ 	265 390	48800 340	—	—	—	−0.33 (2); −0.75 (2)	+1.36 ^[e]
274 ⁺ 	260 340	83000 3000	—	—	—	−0.31 (2) ^[g] ; −0.72 (2) ^[g]	—
174 ⁺ 	273 561	29300 1100	—	—	—	−0.57 (2); −0.97 (2)	+1.08 ^[e] ; +1.35 ^[e] ; +1.54 ^[e]
224 ⁺ 	280 535	58300 1100	—	—	—	−0.48 (2); −0.87 (2)	+1.12 ^[e] ; +1.3 ^[e] ; +1.53 ^[e]
244 ⁺ 	283 549	62400 1400	—	—	—	−0.50 (2); −0.89 (2)	+1.06 ^[e] ; +1.18 ^[e] ; +1.53 ^[e]
184 ⁺ 	273 564	50500 1900	—	—	—	−0.55 (2); −0.98 (2)	+1.07 ^[e] ; +1.34 ^[e]
284 ⁺ 	266 558	83000 1300	—	—	—	−0.55 (2) ^[i] ; −0.90 (2) ^[i]	+1.08 ^[e] ; +1.34 ^[e]
294 ⁺ 	275 540	80000 1100	—	—	—	−0.45 (2) ^[g] ; −0.82 (2) ^[g]	+1.07 ^[e,g] ; +1.12 ^[e,g] ; +1.23 ^[e,g] ; +1.51 ^[e,g]

[a] Argon purged solution, TBAPF₆ as supporting electrolyte, glassy carbon as working electrode; $E_{1/2}$ in V vs SCE, unless otherwise noted; for reversible processes, the number of exchanged electrons is indicated in parentheses. [b] λ_{ex} = 295 nm. [c] Measured on very dilute solutions using naphthalene in degassed cyclohexane as a standard (Φ =0.23; see Ref. 22). [d] Model compound. [e] Poorly reversible process; potential value estimated from DPV peaks. [f] In agreement with the results reported in Ref. 14. [g] Data from Ref. 15. [h] Very broad DPV peak. [i] In agreement with the results reported in Ref. 16.

dergoes^[18] two bielectron reduction processes at −0.29 and −0.71 V.

Macrocyclic Polyethers: The macrocyclic polyether **4** shows (Table 2) two distinct oxidation processes. The first process occurs at a potential slightly less positive than that of 1,5-dimethoxynaphthalene and it can be assigned to the oxidation of one of the two 1,5-dioxynaphthalene units which, since the macrocyclic polyether is very flexible, can

be stabilized by a donor-acceptor interaction with the not yet oxidized unit. As a consequence, oxidation of the second 1,5-dioxynaphthalene unit is displaced to a more positive potential (it should also be considered that second oxidation is disfavored by electrostatic repulsion). The macrocyclic polyether **5**, which contains three equivalent 1,5-dioxynaphthalene units, shows three distinct oxidation processes. The first process occurs at a less positive value

than that of 1,5-dimethoxynaphthalene and also of **4**, which has been accounted for by the formation in **5** of a stabilized structure where the oxidized unit is sandwiched between the two non-oxidized ones. The second process occurs at the same potential as for **4**, suggesting that, in the dioxidized species, the macrocyclic polyether has a geometry that does not allow electronic interactions between the unoxidized and oxidized units. The third oxidation process is, as expected, strongly displaced to more positive potentials. The macrocyclic polyether **6**, which contains four equivalent 1,5-dioxynaphthalene units, shows only two oxidation processes, the second of which corresponds to a very broad DPV peak. Since these processes are poorly reversible, it is not possible to say how many electrons are involved. It seems likely that each process corresponds to the oxidation of a couple of units.

Cyclophanes: Cyclophanes **2**⁴⁺, **3**⁴⁺, and **27**⁴⁺, which contain two bipyridinium-type units, exhibit two bielectronic reduction processes. Both processes move to slightly less negative potentials along the series **2**⁴⁺, **3**⁴⁺, and **27**⁴⁺ (Table 2). Discussion of this trend is made difficult because these compounds do not constitute a homogeneous family. For example, since the 1,5-dioxynaphthalene units contained in **3**⁴⁺ would be better electron donors than the 1,4-dioxybenzene units contained in **2**⁴⁺ (see also the relative position of the intramolecular CT bands, Figure 6, inset), one would expect that the bipyridinium units of **3**⁴⁺ were reduced at more negative potentials than those of **2**⁴⁺ because of a stronger intramolecular CT interaction. The result obtained, however, shows that other factors (e.g., geometrical constraints) must be involved. It should be noted that oxidation of the dioxybenzene and dioxynaphthalene units of the cyclophanes occurs at much higher potentials than for 1,4-dimethoxybenzene and 1,5-dimethoxynaphthalene – or for macrocyclic polyethers like **4** and its dimethoxybenzene analogue^[18] – because of the electron donor-acceptor interaction with the bipyridinium units. The potential values for such oxidation processes are very similar to those observed for these units when they occupy an “alongside” position in [2]catenanes.^[14b,18] No oxidation process can be observed for **27**⁴⁺ because biphenyl undergoes oxidation at very positive potentials.^[17]

[3]Catenanes: The redox patterns of the [3]catenanes are very complex, as expected for systems containing many interacting electroactive units. On the oxidation side, it is not possible to establish the number of electrons exchanged in the various processes because of their poor reversibility. Therefore, we would only like to draw attention to the fact that, in all compounds, there is a first oxidation process around +1.1 V, which is an unusually low potential value for a CT-interacting dioxynaphthalene unit. We suggest that such a process involves oxidation of an “inside” dioxynaphthalene unit which can then be stabilized by CT interaction with the other dioxynaphthalene unit facing it. The second oxidation process, taking place around +1.3 V for **17**⁴⁺, **22**⁴⁺, **18**⁴⁺, and **28**⁴⁺, is most probably associated with oxidation of “alongside” dioxynaphthalene units. The third oxidation process around +1.5 V, observed for **17**⁴⁺, **22**⁴⁺,

and **24**⁴⁺, could involve the dioxybenzene units that are present in such compounds. The second oxidation process at +1.18 V for **24**⁴⁺ is most likely associated with oxidation of the almost non-interacting dioxynaphthalene units of the very large macrocyclic polyether **6**. The oxidation processes that follow the first one in the case of **29**⁴⁺ are difficult to assign. As far as reduction is concerned, the results obtained are much more reliable because of the full reversibility of the observed processes and are also much easier to rationalize because of the fewer units involved. First of all, it should be pointed out that, for each compound, only two distinct bielectronic processes are observed. This observation establishes that the two bipyridinium units are more or less equivalent, both in the original compounds and in their two- and four-electron reduced forms, suggesting that the compounds exhibit highly symmetric structures, probably not unlike those shown in the cartoons illustrated in Figure 4.

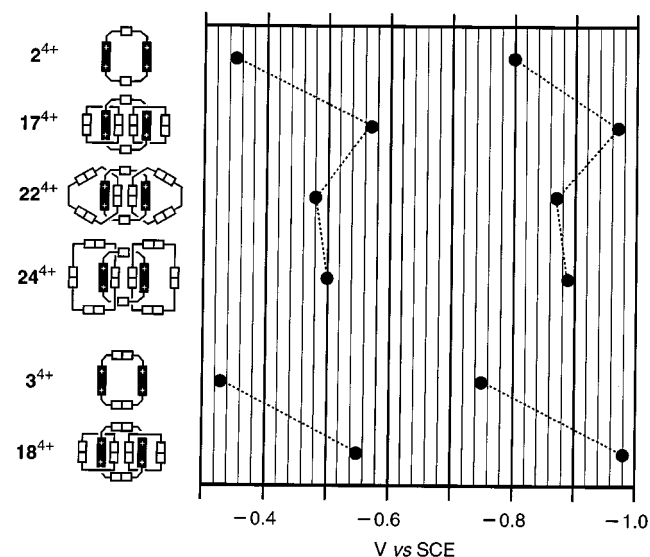


Figure 7. Correlation diagram for the reduction processes of some of the examined compounds

The data collected in Table 2 and schematically represented in Figure 7 for cyclophanes **2**⁴⁺ and **3**⁴⁺ and their [3]catenanes allow us to draw several important conclusions.

(a) Catenation causes the displacement of the reduction processes toward more negative potentials, as expected because of the intercomponent CT interaction. The first reduction process is more affected than the second one because of the lower acceptor power of the reduced bipyridinium units.

(b) For the catenanes derived from cyclophane **2**⁴⁺, **17**⁴⁺ shows the strongest displacement of the reduction processes, presumably because the small size of the macrocyclic polyether **4** favors donor/acceptor interactions.

(c) In the same family, the reduction potential is slightly more negative for **24**⁴⁺ than for **22**⁴⁺, indicating that the larger, symmetric, and more flexible macrocyclic polyether **6** is more prone than the smaller, non-symmetric, and less

flexible macrocyclic polyether **5** to undergo CT interactions with the bipyridinium units of cyclophane **2**⁴⁺.

(*d*) Comparison between catenanes **17**⁴⁺ and **18**⁴⁺, which contain the same macrocyclic polyether **4** together with the cyclophanes **2**⁴⁺ and **3**⁴⁺, respectively, shows that the second process is noticeably more displaced toward negative potentials in the case of **18**⁴⁺. The reason for this observation is most likely related to the bulkiness of the dioxynaphthalene groups which can favor structures where the monoreduced acceptor units of the cyclophane can still interact intimately with the donor units of the crowns.

(*e*) For catenanes **28**⁴⁺ and **29**⁴⁺, which contain the cyclophane **27**⁴⁺, the observed trend is the same as that shown by **17**⁴⁺ and **22**⁴⁺ (point *b* above).

Conclusion

Tetracationic cyclophanes, composed of two bipyridinium units separated by dioxyarene-based spacers, can be incorporated into mechanically-interlocked molecules with the assistance of 1,5-dioxynaphthalene-based macrocyclic polyether templates. This template-directed synthetic approach has been employed to self-assemble [*n*]catenanes, incorporating from two up to seven macrocyclic components. The number of interlocked macrocycles within each catenane can be determined by mass spectrometry, using a variety of ionization techniques – namely, liquid secondary ion, matrix-assisted laser desorption ionization, and/or electrospray. It is interesting to note that the high molecular weight [5]- and [7]catenanes could only be analyzed by electrospray mass spectrometry. The interlocked structure of one of the [3]catenanes was characterized also by single crystal X-ray analysis which revealed the formation of infinite polar stacks in the solid state.

The absorption spectra of the tetracationic cyclophanes incorporating both electron-donor and electron-acceptor units exhibit intramolecular CT absorption bands, whereas in the [3]catenanes that contain these tetracationic cyclophanes interlocked with two macrocyclic polyethers bearing two, three, or four dioxynaphthalene-type units, inter-component CT bands can be observed. The low energy CT excited states are responsible for the lack of fluorescence for cyclophanes and catenanes. The electrochemical behavior of the cyclophanes, macrocyclic polyethers, and catenanes is very complicated because of the presence of many, mutually interacting, electroactive units. In the catenanes, the reduction processes occur at more negative potentials than in the case of the free tetracationic cyclophanes. These changes are a result of the intracatenane CT interactions and their magnitude is related to the sizes and flexibilities of the interlocked macrocycles.

Experimental Section

General Methods: Chemicals were purchased from Aldrich and used as received. Solvents were dried according to literature proced-

ures.^[19] The compounds **4**·**12**·2 PF₆ and **17**·**4** PF₆ were prepared as described^[1,5,10] previously in the literature. – Reactions were carried out in Teflon vessels using a custom-built ultrahigh pressure reactor manufactured by PSIKA Pressure Systems Limited of Glossop, UK. – Thin layer chromatography (TLC) was carried out on aluminum sheets coated with silica-gel 60 (Merck 5554). Column chromatography was performed on silica-gel 60 (Merck 9385, 230–400 mesh). – Melting points were determined on an Electrothermal 9200 melting point apparatus and are uncorrected. – Liquid secondary ion mass spectrometry (LSIMS) was performed on a VG Zabspec instrument using 3-nitrobenzyl alcohol as matrix. Matrix-assisted laser desorption ionization/time-of-flight mass spectrometry (MALDI-TOFMS) was performed on a Kratos Kompact MALDI-III instrument, using either gentisic acid as matrix. Electrospray mass spectra (ESMS) were measured on a VG Prospec mass spectrometer. – ¹H- and ¹³C-NMR spectra were recorded on Bruker AC300 or AMX400 spectrometers. – Elemental analyses were performed by Quantitative Technologies Inc.

Photophysical and Electrochemical Experiments: The equipment and procedures used for absorption, luminescence, and electrochemical measurements have been previously reported.^[20] The standard used for luminescence quantum yield measurements was naphthalene in degassed cyclohexane ($\Phi = 0.23$).^[21] For the electrochemical experiments described in this work, it should be noted that the concentration of the electroactive species was of the order of 10^{−4} mol L^{−1} while 0.05 mol L^{−1} tetraethylammonium hexafluorophosphate was added as supporting electrolyte, and ferrocene was used as internal reference.^[22] Cyclic voltammograms (CV) were obtained at sweep rates of 10, 20, 50, 100, 200, 500, and 1000 mV s^{−1} whereas differential pulse voltammograms (DPV) were performed with scan rates of 20 or 4 mV s^{−1}, a pulse height of 75 or 10 mV, and a duration of 40 ms. For reversible processes the same halfwave potential values were obtained from the DPV peaks and from an average of the cathodic and anodic cyclic voltammetric peaks. The potential values for not fully-reversible processes were estimated from the DPV peaks. The experimental error on the potential values for reversible and not fully-reversible processes was estimated to be ± 5 and ± 10 mV, respectively.

[2]Catenane 13·4 PF₆ and [3]Catenane 16·4 PF₆: A solution of **4** (74.4 mg, 0.12 mmol), **7** (29.8 mg, 0.09 mmol), and **10**·2 PF₆ (36.0 mg, 0.05 mmol) in DMF (15 mL) was subjected to a pressure of 12 kbar for 5 d at 20 °C. The solvent was distilled off under reduced pressure and the residue was purified by column chromatography [SiO₂: MeOH/2 M NH₄Cl_{aq}/MeNO₂ (7:2:1)] to afford two products which were dissolved in H₂O. The precipitates, obtained after the addition of NH₄PF₆, were filtered off and dried to afford the [2]catenane **13**·4 PF₆ (5.5 mg, 6%) and the [3]catenane **16**·4 PF₆ (0.7 mg, 1%) as red solids. – **13**·4 PF₆: LSIMS: *m/z* = 1711 [M – PF₆]⁺, 1566 [M – 2 PF₆]⁺, 1421 [M – 3 PF₆]⁺. – ¹H-NMR [300 MHz, (CD₃)₂CO, 298 K]: δ = 9.13 (8 H, bs), 7.85 (8 H, bs), 7.35 (2 H, t, *J* = 8.0 Hz), 7.25–7.20 (4 H, m), 7.03 (2 H, t, *J* = 2.3 Hz), 6.95–6.60 (12 H, m), 5.45–5.40 (8 H, m), 4.80–4.75 (8 H, m), 4.15–4.10 (8 H, m), 3.98–3.90 (16 H, m), 3.85–3.80 (8 H, m). – **16**·4 PF₆: LSIMS: *m/z* = 2349 [M – PF₆]⁺, 2204 [M – 2 PF₆]⁺, 2059 [M – 3 PF₆]⁺, 1913 [M – 4 PF₆]⁺.

[3]Catenane 18·4 PF₆: A solution of **4** (101.0 mg, 0.16 mmol), **9** (30.3 mg, 0.08 mmol), and **12**·2 PF₆ (54.4 mg, 0.07 mmol) in DMF (15 mL) was subjected to a pressure of 12 kbars for 5 d at 20 °C. The solvent was distilled off under reduced pressure and the residue was purified by column chromatography [SiO₂: MeOH/2 M NH₄Cl_{aq}/MeNO₂ (7:2:1)] to afford a purple solid which was dissolved in H₂O. The precipitate, obtained after the addition of

NH_4PF_6 , was filtered off and dried to afford the [3]catenane **18** · 4 PF_6 (7.0 mg, 4%) as a purple solid. – **18** · 4 PF_6 : LSIMS: $m/z = 2594 [\text{M}]^+$, 2449 $[\text{M} - \text{PF}_6]^+$, 2304 $[\text{M} - 2 \text{PF}_6]^+$, 2159 $[\text{M} - 3 \text{PF}_6]^+$. – ^1H NMR [400 MHz, $(\text{CD}_3)_2\text{CO}$, 233 K]: $\delta = 8.82$ (4 H, d, $J = 6.3$ Hz), 8.74 (4 H, d, $J = 6.5$ Hz), 8.09 (4 H, d, $J = 8.4$ Hz), 7.59 (4 H, t, $J = 8.2$ Hz), 7.25 (4 H, d, $J = 5.7$ Hz), 7.13–7.10 (8 H, m), 6.96 (4 H, t, $J = 8.0$ Hz), 6.60 (4 H, d, $J = 5.3$ Hz), 6.31 (4 H, d, $J = 7.6$ Hz), 5.76–5.69 (8 H, m), 5.44 (4 H, d, $J = 7.5$ Hz), 5.19 (4 H, t, $J = 12.4$ Hz), 5.03 (4 H, t, $J = 11.1$ Hz), 4.81 (4 H, d, $J = 9.5$ Hz), 4.50 (4 H, d, $J = 8.1$ Hz), 4.00–3.49 (64 H, m). – ^{13}C NMR (101 MHz, CD_3CN , 348 K): $\delta = 154.7, 153.8, 145.9, 144.4, 127.6, 126.6, 126.6, 126.1, 124.5, 116.6, 115.0, 107.2, 105.9, 72.7, 72.4, 71.5, 69.3, 68.3, 62.8$. – Crystal data: $[\text{C}_{120}\text{H}_{132}\text{N}_4\text{O}_{24}][\text{PF}_6]_4 \cdot 2.5 \text{ MeCN} \cdot \text{H}_2\text{O}$, $M = 2714.8$, monoclinic, space group $C2/c$ (no. 15), $a = 39.341(5)$, $b = 24.897(1)$, $c = 31.028(5)$ Å, $\beta = 107.37(1)^\circ$, $V = 29005(6)$ Å³, $Z = 8$, $\rho_c = 1.243$ g cm^{−3}, $\mu(\text{Cu}_{\text{K}\alpha}) = 13.1$ cm^{−1}, $F(000) = 11304$, $T = 203$ K; brown tabular prisms, $0.57 \times 0.43 \times 0.30$ mm, Siemens P4 rotating anode diffractometer, graphite-monochromated $\text{Cu}_{\text{K}\alpha}$ radiation, ω -scans, 16024 independent reflections. The structure was solved by direct methods and the major occupancy non-hydrogen atoms of the [3]catenane and of the hexafluorophosphate counterions were refined anisotropically (the others isotropically) using blocked full matrix least-squares based on F^2 to give $R_1 = 0.260$, $wR_2 = 0.580$ for 6212 independent observed reflections $[|F_o| > 4\sigma(|F_o|)]$, $2\theta \leq 105^\circ$ and 1595 parameters. The very high value of R_1 is a result of a combination of very weak data from a partially crazed crystal and the significant disorder associated with the hexafluorophosphate counterions (which are distributed over six partial occupancy sites) and with the included solvent molecules. However, the geometry of the [3]catenane is generally well resolved though here is evidence for “pedaling” of one of the “alongside” 1,5-dioxynaphthalene ring systems (two discrete orientations for this unit were identified and refined). Crystallographic data (excluding structure factors) for the structure reported in this paper have been deposited with the Cambridge Crystallographic Data Centre as supplementary publication no. CCDC-134656.

[2]Catenane 19 · 4 PF_6 : A solution of **5** (110.0 mg, 0.12 mmol), **7** (26.4 mg, 0.08 mmol), and **10** · 2 PF_6 (36.0 mg, 0.05 mmol) in DMF (15 mL) was subjected to a pressure of 12 kbars for 5 d at 20 °C. The solvent was distilled off under reduced pressure and the residue was purified by column chromatography [SiO_2 : MeOH/2M $\text{NH}_4\text{Cl}_{\text{aq}}/\text{MeNO}_2$ (7:2:1)] to afford a purple solid which was dissolved in H_2O . The precipitate, obtained after the addition of NH_4PF_6 , was filtered off and dried to afford the [2]catenane **19** · 4 PF_6 (25.1 mg, 26%) as a red solid. – **19** · 4 PF_6 : LSIMS: $m/z = 2175 [\text{M}]^+$, 2030 $[\text{M} - \text{PF}_6]^+$, 1885 $[\text{M} - 2 \text{PF}_6]^+$, 1739 $[\text{M} - 3 \text{PF}_6]^+$. – ^1H NMR [400 MHz, $(\text{CD}_3)_2\text{CO}$, 304 K]: $\delta = 9.05$ (8 H, d, $J = 7.0$ Hz), 7.75 (8 H, d, $J = 7.0$ Hz), 7.26 (6 H, d, $J = 8.5$ Hz), 7.24 (2 H, t, $J = 8.6$ Hz), 6.97 (6 H, t, $J = 8.0$ Hz), 6.81 (2 H, t, $J = 2.3$ Hz), 6.69 (6 H, d, $J = 7.7$ Hz), 6.64 (4 H, dd, $J = 8.4$ Hz, $J = 2.4$ Hz), 5.25 (8 H, t, $J = 4.3$ Hz), 4.61 (8 H, t, $J = 4.4$ Hz), 4.13–4.11 (12 H, m), 3.91–3.89 (12 H, m), 3.81–3.78 (24 H, m). – ^{13}C NMR [400 MHz, $(\text{CD}_3)_2\text{CO}$, 304 K]: $\delta = 159.2, 154.4, 147.8, 146.6, 131.3, 126.6, 126.1, 125.8, 114.5, 106.6, 104.7, 71.2, 70.8, 70.2, 68.7, 66.6, 61.8$.

[3]Catenane 22 · 4 PF_6 : A solution of **5** (240.0 mg, 0.25 mmol), **8** (33.0 mg, 0.10 mmol), and **11** · 2 PF_6 (77.0 mg, 0.10 mmol) in DMF (15 mL) was subjected to a pressure of 12 kbars for 5 d at 20 °C. The solvent was distilled off under reduced pressure and the residue was purified by column chromatography [SiO_2 : MeOH/2M $\text{NH}_4\text{Cl}_{\text{aq}}/\text{MeNO}_2$ (7:2:1)] to afford a purple solid which was dis-

solved in H_2O . The precipitate, obtained after the addition of NH_4PF_6 , was filtered off and dried to afford the [3]catenane **22** · 4 PF_6 (64.4 mg, 21%) as a purple solid. – **22** · 4 PF_6 : LSIMS: $m/z = 2983 [\text{M} - \text{PF}_6]^+$, 2838 $[\text{M} - 2 \text{PF}_6]^+$, 2693 $[\text{M} - 3 \text{PF}_6]^+$. – ^1H NMR [400 MHz, $(\text{CD}_3)_2\text{CO}$, 304 K]: $\delta = 8.62$ (8 H, d, $J = 7.0$ Hz), 7.08 (8 H, s), 7.03 (8 H, d, $J = 7.0$ Hz), 6.86–6.58 (24 H, m), 6.42–6.22 (12 H, m), 5.08–5.00 (8 H, m), 4.55–4.49 (8 H, m), 3.98–3.89 (24 H, m), 3.85–3.74 (24 H, m), 3.72–3.64 (48 H, m).

[2]Catenane 23 · 4 PF_6 , [3]Catenane 24 · 4 PF_6 , [5]Catenane 25 · 8 PF_6 , and [7]Catenane 26 · 12 PF_6 : A solution of **6** (141.0 mg, 0.11 mmol), **8** (33.0 mg, 0.10 mmol), and **11** · 2 PF_6 (33.2 mg, 0.054 mmol) in DMF (15 mL) was subjected to a pressure of 12 kbars for 5 d at 20 °C. The solvent was distilled off under reduced pressure and the residue was purified by column chromatography [SiO_2 : MeOH/2M $\text{NH}_4\text{Cl}_{\text{aq}}/\text{MeNO}_2$ (7:2:1)] to afford four products which were dissolved in H_2O . The precipitates, obtained after the addition of NH_4PF_6 , were filtered off and dried to afford the [2]catenane **23** · 4 PF_6 (5.0 mg, 5%), the [3]catenane **24** · 4 PF_6 (22.1 mg, 14%), the [5]catenane **25** · 8 PF_6 (10.0 mg, 4%), and the [7]catenane **26** · 12 PF_6 (8.3 mg, 2%) as purple solids. – **23** · 4 PF_6 : LSIMS: $m/z = 2349 [\text{M} - \text{PF}_6]^+$, 2204 $[\text{M} - 2 \text{PF}_6]^+$, 2059 $[\text{M} - 3 \text{PF}_6]^+$. – MALDI-TOFMS: $m/z = 2201 [\text{M} - 2 \text{PF}_6]^+$, 2057 $[\text{M} - 3 \text{PF}_6]^+$, 1913 $[\text{M} - 4 \text{PF}_6]^+$. – ESMS: $m/z = 2348 [\text{M} - \text{PF}_6]^+$, 1102 $[\text{M} - 2 \text{PF}_6]^{2+}$, 686 $[\text{M} - 3 \text{PF}_6]^{3+}$. – ^1H NMR [300 MHz, $(\text{CD}_3)_2\text{CO}$, 298 K]: $\delta = 8.91$ (8 H, d, $J = 6.6$ Hz), 7.86 (8 H, d, $J = 6.3$ Hz), 7.17 (8 H, d, $J = 8.5$ Hz), 6.87 (8 H, t, $J = 8.1$ Hz), 6.63 (8 H, s), 6.49 (8 H, d, $J = 7.7$ Hz), 5.15 (8 H, m), 4.38 (8 H, m), 4.01–3.99 (16 H, m), 3.89–3.87 (16 H, m), 3.80–3.79 (32 H, m). – ^{13}C NMR [101 MHz, $(\text{CD}_3)_2\text{CO}$, 298 K]: $\delta = 154.7, 153.2, 146.6, 126.9, 126.2, 125.8, 116.0, 114.7, 106.6, 71.5, 71.2, 70.4, 68.8, 67.3, 62.1$. – **24** · 4 PF_6 : LSIMS: $m/z = 3621 [\text{M} - \text{PF}_6]^+$, 3477 $[\text{M} - 2 \text{PF}_6]^+$, 3332 $[\text{M} - 3 \text{PF}_6]^+$, 3186 $[\text{M} - 4 \text{PF}_6]^+$. – MALDI-TOFMS: $m/z = 3335 [\text{M} - 3 \text{PF}_6]^+$, 3191 $[\text{M} - 4 \text{PF}_6]^+$. – ESMS: $m/z = 2868 [4 \text{M} - 5 \text{PF}_6]^{5+}$, 2680 $[3 \text{M} - 4 \text{PF}_6]^{4+}$, 2367 $[2 \text{M} - 3 \text{PF}_6]^{3+}$, 1739 $[\text{M} - 2 \text{PF}_6]^{2+}$, 1111 $[\text{M} - 3 \text{PF}_6]^{3+}$, 797 $[\text{M} - 4 \text{PF}_6]^{4+}$. – ^1H NMR (300 MHz, CD_3CN , 344 K): $\delta = 8.25$ (8 H, d, $J = 6.8$ Hz), 6.94 (8 H, s), 6.93–6.84 (32 H, m), 6.50 (8 H, d, $J = 7.0$ Hz), 6.37 (16 H, d, $J = 7.5$ Hz), 4.80 (8 H, bs), 4.39 (8 H, bs), 3.94–3.92 (32 H, m), 3.83–3.81 (32 H, m), 3.73–3.71 (64 H, m). – ^{13}C NMR [101 MHz, $(\text{CD}_3)_2\text{CO}$, 304 K]: $\delta = 154.3, 153.2, 145.6, 144.3, 126.7, 126.0, 124.3, 115.6, 114.6, 106.0, 71.5, 71.4, 70.5, 68.6, 67.4, 62.2$. – **25** · 8 PF_6 : ESMS: $m/z = 1941 [\text{M} - 3 \text{PF}_6]^{3+}$, 1420 $[\text{M} - 4 \text{PF}_6]^{4+}$, 1107 $[\text{M} - 5 \text{PF}_6]^{5+}$, 898 $[\text{M} - 6 \text{PF}_6]^{6+}$, 749 $[\text{M} - 7 \text{PF}_6]^{7+}$, 637 $[\text{M} - 8 \text{PF}_6]^{8+}$. – ^1H NMR (400 MHz, CD_3CN , 348 K): $\delta = 8.50$ –8.35 (16 H, m), 6.98 (16 H, s), 6.95–6.93 (16 H, m), 6.86 (16 H, t, $J = 7.8$ Hz), 6.80 (8 H, d, $J = 7.0$ Hz), 6.75–6.60 (8 H, m), 6.45 (8 H, m), 6.40 (16 H, d, $J = 7.6$ Hz), 6.18–6.10 (8 H, m), 6.04 (8 H, d, $J = 7.6$ Hz), 4.90 (16 H, bs), 4.43 (16 H, bs), 3.96–3.94 (64 H, m), 3.83–3.79 (64 H, m), 3.75–3.72 (64 H, m). – **26** · 12 PF_6 : ESMS: $m/z = 2043 [\text{M} - 4 \text{PF}_6]^{4+}$, 1606 $[\text{M} - 5 \text{PF}_6]^{5+}$, 1314 $[\text{M} - 6 \text{PF}_6]^{6+}$, 1105 $[\text{M} - 7 \text{PF}_6]^{7+}$, 949 $[\text{M} - 8 \text{PF}_6]^{8+}$, 828 $[\text{M} - 9 \text{PF}_6]^{9+}$, 730 $[\text{M} - 10 \text{PF}_6]^{10+}$.

Acknowledgments

This research was supported by the European Community within the Training and Mobility of Researchers program (Marie Curie grant for Dr. H. D. A. Hoffmann), contract FMRX-CT96-0076, MURST (Supramolecular Devices Project), and the University of Bologna (Funds for Selected Topics).

[1] [1a] P. R. Ashton, C. G. Claessens, W. Hayes, S. Menzer, J. F. Stoddart, A. J. P. White, D. J. Williams, *Angew. Chem. Int. Ed.*

- 1995, 34, 1862–1865. – [11b] P. R. Ashton, A. Chemin, C. G. Claessens, S. Menzer, J. F. Stoddart, A. J. P. White, D. J. Williams, *Eur. J. Org. Chem.* **1998**, 969–981.
- [2] For accounts and reviews on $[\pi\cdots\pi]$ stacking interactions, see: [2a] M. H. Schwartz, *J. Inclusion Phenom.* **1990**, 9, 1–35. – [2b] J. H. Williams, *Acc. Chem. Res.* **1993**, 26, 593–598; C. A. Hunter, *Angew. Chem. Int. Ed.* **1993**, 32, 1584–1586. – [2c] C. A. Hunter, *J. Mol. Biol.* **1993**, 230, 1025–1054. – [2d] T. Dahl, *Acta Chem. Scand.* **1994**, 48, 95–116. – [2e] F. Cozzi, J. S. Siegel, *Pure Appl. Chem.* **1995**, 67, 683–689. – [2f] C. G. Claessens, J. F. Stoddart, *J. Phys. Org. Chem.* **1997**, 10, 254–272.
- [3] For examples of self-complementary molecules, see: [3a] J. Rebek Jr., *Angew. Chem. Int. Ed.* **1990**, 29, 245–255. – [3b] S. Hoffmann, *Angew. Chem. Int. Ed.* **1992**, 31, 1013–1016. – [3c] L. E. Orgel, *Nature* **1992**, 358, 203–209. – [3d] E. A. Winter, M. M. Conn, J. Rebek Jr., *Acc. Chem. Res.* **1994**, 27, 198–203. – [3e] L. E. Orgel, *Acc. Chem. Res.* **1995**, 28, 109–118. – [3f] J. L. Atwood, K. T. Holman, J. W. Steed, *Chem. Commun.* **1996**, 1401–1407. – [3g] J. Rebek Jr., *Chem. Soc. Rev.* **1996**, 25, 255–264. – [3h] S. Kauffman, *Nature* **1996**, 382, 496–497. – [3i] M. M. Conn, J. Rebek Jr., *Chem. Rev.* **1997**, 97, 1647–1668. – [3j] D. H. Lee, K. Severin, M. R. Ghadiri, *Curr. Op. Chem. Biol.* **1997**, 1, 491–496. – [3k] P. R. Ashton, I. Baxter, S. J. Cantrill, M. C. T. Fyfe, P. T. Glink, J. F. Stoddart, A. J. P. White, D. J. Williams, *Angew. Chem. Int. Ed.* **1998**, 37, 1294–1297. – [3l] P. R. Ashton, I. W. Parsons, F. M. Raymo, J. F. Stoddart, A. J. P. White, D. J. Williams, R. Wolf, *Angew. Chem. Int. Ed.* **1998**, 37, 1913–1916. – [3m] J. Rebek Jr., *Acc. Chem. Res.* **1999**, 32, 278–286. – [3n] N. Yamaguchi, H. W. Gibson, *Angew. Chem. Int. Ed.* **1999**, 38, 143–147. – [3o] A. R. Renslo, D. M. Rudkevich, J. Rebek Jr., *J. Am. Chem. Soc.* **1999**, 121, 7459–7460. – [3p] J. Cabezon, J. Cao, F. M. Raymo, J. F. Stoddart, A. J. P. White, D. J. Williams, *Angew. Chem. Int. Ed.* **2000**, 39, 148–151.
- [4] P. Laitenberger, C. G. Claessens, L. Kuipers, F. M. Raymo, R. E. Palmer, J. F. Stoddart, *Chem. Phys. Lett.* **1997**, 279, 209–214.
- [5] P. R. Ashton, S. E. Boyd, C. G. Claessens, R. E. Gillard, S. Menzer, J. F. Stoddart, M. S. Tolley, A. J. P. White, D. J. Williams, *Chem. Eur. J.* **1997**, 3, 788–798.
- [6] For accounts and reviews on $[C-H\cdots O]$ hydrogen bonds, see: [6a] G. R. Desiraju, *Acc. Chem. Res.* **1991**, 24, 290–296. – [6b] G. R. Desiraju, *Acc. Chem. Res.* **1996**, 29, 441–449. – [6c] T. Steiner, *Chem. Commun.* **1997**, 727–734. – [6d] I. Berger, M. Egli, *Chem. Eur. J.* **1997**, 3, 1400–1404.
- [7] For accounts and reviews on $[C-H\cdots\pi]$ interactions, see: [7a] M. Oki, *Acc. Chem. Res.* **1990**, 23, 351–356. – [7b] M. C. Etter, *J. Phys. Chem.* **1991**, 95, 4601–4610. – [7c] M. J. Zaworotko, *Chem. Soc. Rev.* **1994**, 23, 283–288. – [7d] M. Nishio, Y. Umezawa, M. Hirota, Y. Takeuchi, *Tetrahedron* **1995**, 51, 8665–8701. – [7e] M. Nishio, Y. Umezawa, M. Hirota, *The [C-H \cdots π] Interaction*, Wiley-VCH, New York, **1998**.
- [8] For accounts and reviews on catenanes and rotaxanes having intercomponent $[C-H\cdots O]$ hydrogen bonds, $[\pi\cdots\pi]$ stacking, and $[C-H\cdots\pi]$ interactions, see: [8a] D. Pasini, F. M. Raymo, J. F. Stoddart, *Gazz. Chim. Ital.* **1995**, 125, 431–435. – [8b] D. B. Amabilino, F. M. Raymo, J. F. Stoddart, *Comprehensive Supramolecular Chemistry*, Vol. 9 (Eds.: M. W. Hosseini, J.-P. Sauvage), Pergamon, Oxford, **1996**, 85–130. – [8c] R. E. Gillard, F. M. Raymo, J. F. Stoddart, *Chem. Eur. J.* **1997**, 3, 1933–1940. – [8d] F. M. Raymo, J. F. Stoddart, *Chemtracts* **1998**, 11, 491–511.
- [9] For books and reviews on catenanes and rotaxanes, see: [9a] J.-C. Chambron, C. O. Dietrich-Buchecker, J.-P. Sauvage, *Top. Curr. Chem.* **1993**, 165, 131–162. – [9b] H. W. Gibson, H. Marand, *Adv. Mater.* **1993**, 5, 11–21. – [9c] H. W. Gibson, M. C. Bheda, P. T. Engen, *Prog. Polym. Sci.* **1994**, 19, 843–945. – [9d] D. B. Amabilino, J. F. Stoddart, *Chem. Rev.* **1995**, 95, 2725–2828. – [9e] M. Belohradsky, F. M. Raymo, J. F. Stoddart, *Collect. Czech. Chem. Commun.* **1996**, 61, 1–43 and 527–557. – [9f] M. Fujita, K. Ogura, *Coord. Chem. Rev.* **1996**, 148, 249–264. – [9g] R. Jäger, F. Vögtle, *Angew. Chem. Int. Ed.* **1997**, 36, 930–944. – [9h] S. A. Nepogodiev, J. F. Stoddart, *Chem. Rev.* **1998**, 98, 1959–1976. – [9i] M. Fujita, *Acc. Chem. Res.* **1999**, 32, 53–61. – [9j] D. A. Leigh, A. Murphy, *Chem. Ind.* **1999**, 178–183. – [9k] F. M. Raymo, J. F. Stoddart, *Chem. Rev.* **1999**, 99, 1643–1664. – [9l] *Molecular Catenanes, Rotaxanes and Knots* (Eds.: J.-P. Sauvage, C. O. Dietrich-Buchecker), VCH-Wiley, Weinheim, **1999**. – [9m] G. A. Breault, C. A. Hunter, P. C. Mayers, *Tetrahedron* **1999**, 55, 5265–5293.
- [10] D. B. Amabilino, P. R. Ashton, S. E. Boyd, J. Y. Lee, S. Menzer, J. F. Stoddart, D. J. Williams, *Angew. Chem. Int. Ed. Engl.* **1997**, 36, 2070–2072.
- [11] For related [2]catenanes incorporating 1,5-dioxynaphthalene recognition sites, see: [11a] D. G. Hamilton, J. K. M. Sanders, J. E. Davies, W. Clegg, S. J. Teat, *Chem. Commun.* **1997**, 897–898. – [11b] A. C. Try, M. M. Harding, D. G. Hamilton, J. K. M. Sanders, *Chem. Commun.* **1998**, 723–724. – [11c] D. G. Hamilton, J. E. Davies, L. Prodi, J. K. M. Sanders, *Chem. Eur. J.* **1998**, 4, 608–620. – [11d] D. G. Hamilton, N. Feeder, L. Prodi, S. J. Teat, W. Clegg, J. K. M. Sanders, *J. Am. Chem. Soc.* **1998**, 120, 1096–1097. – [11e] D. G. Hamilton, N. Feeder, S. J. Teat, J. K. M. Sanders, *New J. Chem.* **1998**, 1019–1021. – [11f] D. G. Hamilton, L. Prodi, N. Feeder, J. K. M. Sanders, *J. Chem. Soc., Perkin Trans. 1* **1999**, 1057–1066.
- [12] For the template-directed synthesis and X-ray structure of the [3]catenane **17** · 4 PF₆, see ref. [5].
- [13] The electrospray mass spectrum of the [7]catenane **26** · 12 PF₆ shows that this molecule incorporates three tetracationic cyclophanes and four macrocyclic polyethers. However, two isomers incorporating this combination of macrocyclic components are possible. One isomer only is illustrated in Scheme 3. It is composed of a linear array of seven interlocked macrocycles. The other possible isomer, instead, has a “central” macrocyclic polyether interlocked simultaneously with three tetracationic cyclophanes which, in turn, are interlocked with one additional macrocyclic polyether each. As a result of the complexity of the problem and of the difficulty in obtaining sufficient amounts of **26** · 12 PF₆, we have not been able to unravel the structure of the [7]catenane by ¹H-NMR spectroscopy.
- [14] [14a] P. R. Ashton, R. Ballardini, V. Balzani, A. Credi, M. T. Gandolfi, D. J.-F. Marquis, S. Menzer, L. Pérez-García, L. Prodi, J. F. Stoddart, M. Venturi, A. J. P. White, and D. J. Williams, *J. Am. Chem. Soc.* **1995**, 117, 11171–11197. – [14b] P. R. Ashton, V. Balzani, J. Becher, A. Credi, M. C. T. Fyfe, G. Matternsteig, S. Menzer, M. Nielsen, F. M. Raymo, J. F. Stoddart, M. Venturi, D. J. Williams, *J. Am. Chem. Soc.* **1999**, 121, 3951–3957.
- [15] D. B. Amabilino, P. R. Ashton, V. Balzani, S. E. Boyd, A. Credi, J. Y. Lee, S. Menzer, J. F. Stoddart, M. Venturi, D. J. Williams, *J. Am. Chem. Soc.* **1998**, 120, 4295–4307.
- [16] P. R. Ashton, C. L. Brown, E. J. T. Chrystal, T. T. Goodnow, A. E. Kaifer, K. P. Parry, A. M. Z. Slawin, N. Spencer, J. F. Stoddart, D. J. Williams, *Angew. Chem. Int. Ed. Engl.* **1991**, 30, 1039–1042.
- [17] [17a] S. L. Murov, I. Chermichael, G. Hug, *Handbook of Photochemistry*, Dekker, New York, **1993**. – [17b] C. K. Mann, K. K. Barnes, *Electrochemical Reactions in Non Aqueous Systems*, Dekker, New York, **1970**.
- [18] P.-L. Anelli, P. R. Ashton, R. Ballardini, V. Balzani, M. Delgado, M. T. Gandolfi, T. T. Goodnow, A. E. Kaifer, D. Philp, M. Pietraszkiewicz, L. Prodi, M. V. Reddington, A. M. Z. Slawin, N. Spencer, J. F. Stoddart, C. Vicent, D. J. Williams, *J. Am. Chem. Soc.* **1992**, 114, 193–218.
- [19] B. S. Furniss, A. J. Hannaford, P. W. G. Smith, A. R. Tatchell, *Practical Organic Chemistry*, Longman, New York, **1989**.
- [20] D. B. Amabilino, P. R. Ashton, V. Balzani, C. L. Brown, A. Credi, J. M. J. Freché, J. W. Leon, F. M. Raymo, N. Spencer, J. F. Stoddart, M. Venturi, *J. Am. Chem. Soc.* **1996**, 118, 12012–12020.
- [21] I. B. Berlman, *Handbook of Fluorescence Spectra of Aromatic Compounds*, Academic Press, London, **1965**.
- [22] D. Dubois, G. Moninot, W. Kutner, M. T. Jones, K. M. Kadish, *J. Phys. Chem.* **1992**, 96, 7137–7145.

Received September 9, 1999

[O99523]